Int. J. Electrochem. Sci., 6 **(2011)** 819 - 829

International Journal of
ELECTROCHEMICAL
SCIENCE
www.electrochemsci.org

Electrocatalytic Oxidation of NADH on Graphene Oxide and Reduced Graphene Oxide Modified Screen-Printed Electrode

Lei Zhang[1], *Yang Li*[1], *Li Zhang*[1], *Da-Wei Li*[1], *Dimitre Karpuzov*[2], *Yi-Tao Long*[1,*]

[1] Shanghai Key Lab of Functional Materials Chemistry, East China University of Science and Technology, Shanghai, 200237, P.R. China
[2] Alberta Centre for Surface Engineering and Science, University of Alberta, Edmonton, AB, T6G 2G6, Canada
[*]E-mail: *ytlong@ecust.edu.cn*

Received: 11 January 2011 / *Accepted:* 9 February 2011 / *Published:* 1 March 2011

A facile method, Graphene Oxide (GO) modified electrochemically pre-anodized screen-printed carbon electrodes (SPCEs), was developed for the determination of nicotinamide adenine dinucleotide (NADH) in neutral aqueous solution. Compared with the bare SPCEs and the reduced Graphene Oxide (rGO) modified SPCEs (rGO/SPCEs), the GO/SPCEs exhibit greatly enhanced electrocatalytic oxidation toward NADH. The scanning electron microscopy (SEM) and X-ray photoelectron spectroscopy (XPS) provide the substantial evidence for the formation of edge-plane sites on the surface of SPCEs, rGO/SPCEs and GO/SPCEs. The GO/SPCEs show the excellent electrochemical character for the determination of NADH in the range from 0.8 to 500 μM with a detection limit of 0.10 μM. The formation of oxidation product NAD^+ was confirmed by *in-situ* UV-Vis spectroelectrochemistry. It shows a great promise for the design of the disposable amperometric biosensor for NADH.

Keywords: Graphene oxide, nicotinamide adenine dinucleotide, screen-printed electrode, biosensors, XPS

1. INTRODUCTION

The development of electrochemical dihydronicotinamide adenine dinucleotide (NADH) sensor has attracted extensive interests because NADH behaves as an essential cofactor in the naturally occurring enzymatic reactions [1]. The NADH and its oxidized form, NAD^+, are ubiquitous bio-molecules found in both eukaryotic and prokaryotic organisms. Known as coenzymes, the two nucleotides transfer hydrogen and electrons from one metabolite to another in many cellular redox

reactions. Particularly, NAD^+ and NADH are involved in cellular energy metabolism, including glycolysis, tricarboxylic acid cycle and oxidative phosphorylation [2]. Consequently, there is a great need to develop a robust detection for NADH. However, direct electrochemical detection by oxidation of NADH to its corresponding oxidized form NAD^+ at bare electrodes is accompanied by very high overpotential at platinum or carbon [3, 4]. Moreover, the strong adsorption of not only NADH itself but also its oxidation NAD^+ leads to electrode surface fouling and, as a consequence, producing a system which lacks sensitivity, reproducibility and stability [5]. Numerous efforts have been devoted to identifying mediators that will accelerate the interfacial electron transfer between NADH and a solid electrode, such as quinone derivatives [6, 7], thionine derivatives [8], diamines [9], ferrocene [10], ruthenium complexes [11], catechols [12], phenazine [13] and L-glutamate [14] derivatives adsorbed onto graphite or as electrodeposited films. Despite the extensive work carried out, these redox mediators still need improvements, mainly in terms of stability and reproducibility because of the water soluble mediator loss from the electrode surface. In this direction, some works employing nanostructured carbon materials such as pyrolytic graphite [15], carbon nanofibers [16, 17], carbon microparticles [18], especially carbon nanotubes [19-21] have been used widely to reduce the high-overpotential for NADH oxidation, to minimize the surface fouling and to improve electron-transfer kinetics without the help of redox mediators due to their edge-plane sites/defects present in the carbon materials. Despite advantages of these carbon nanomaterials, there still has been significant interest in the development of new carbon nanomaterials to accelerate the development of electroanalytical chemistry.

The screen-printing technology has widely been preformed for the fabrication of the mass, disposable, low-cost electrochemical sensors [22]. Normally carbon materials used as the screen-printed mediators are widely applied in electrochemical research for the determination of biological analytes such as glucose [23], NADH [24] and dopamine [25, 26]. Disposable pre-anodized SPCEs have shown highly improved electrocatalytic activity toward NADH [27]. The pre-anodized SPCEs with the introduction of edge plane carbonyl groups has been demonstrated to act similar to an edge plane graphite or carbon nanotubes (CNTs) modified electrode. Graphene, as a two-dimensional macromolecular sheet of carbon atoms with only one atom thickness, has been extensively used in electrochemistry applications in the recent years because of its unique structure and electrical and mechanical characteristics [28-32]. On the other hand, the graphene oxide (GO) and reduced GO (rGO) have the good electrochemical characters due to the oxygen-containing groups in their edge plane sites. Similar with carbon nanotubes, the higher proportion of edge plane defects may lead to more rapid electron transfer [33]. As a novel carbon nanomaterial, using graphene to develop high-performance sensors for biomolecular is highly expected.

Herein, we report a simple, cost-effective, highly sensitive method for the determination of NADH in neutral aqueous solution. The SPCEs were modified by a thin GO film on the working electrode surface after the electrochemical pre-anodizing. Compared with the bare SPCEs and the rGO/SPCEs, the electrocatalytic oxidation toward NADH on the GO/SPCEs enhanced greatly at the low potential of +0.41 V. The formation of edge plane sites on the surface of SPCEs, rGO/SPCEs and GO/SPCEs were characterized by scanning electron microscope (SEM) and X-ray photoelectron spectroscopy (XPS) spectroscopy. Especially, a linear response was obtained in the 3 order of

magnitude by ranging of 0.8~500 μM for NADH with a detection limit of 0.10 μM on the GO/SPCEs, which is of great interest to minimize interferences and for the design of the disposable amperometric biosensor for NADH.

2. EXPERIMENTAL SECTION

2.1. Reagents and apparatus

Carbon ink, silver ink, and silver-silver chloride ink were obtained from Camnano Technology Co., Ltd. Xuzhou, China. Reduced form of β-nicotinamide adenine dinucleotide was purchased from Sigma. All solutions were prepared with Nanopure water (18 MΩ cm^{-1}) from a Millipore MilliQ system. All chemicals used were of analytical grade and used as received without any further purification.

All electrochemical experiments were conducted with a CHI Instruments (CHI 660C) with an integrated screen-printed three electrode device: a carbon working electrode, a carbon counter electrode, and an Ag/AgCl reference electrode. And all experiments were typically conducted at room temperature (25 ± 2ºC). A 0.1 M phosphate buffer (0.05 M NaH_2PO_4 and 0.05 M Na_2HPO_4 adjusted to pH 7.4 containing 0.1 M KCl) solution (PBS) was used throughout since enzyme-catalysed reactions of NADH and NADPH-dependent dehydrogenases are pH dependent with pH 7 and above. Consequently, the pH of 7.4 used in the experiments was selected based on the previous report [34].

The scanning electron micrographs were taken out by using a JEOL JSM6360 LV scanning electron microscope (JEOL Ltd., Tokyo, Japan). X-ray photoelectron spectroscopy (XPS) analysis was carried out on an AXIS HIS 165 spectrometer (Kratos Analytical) using a monochromatized Al Kr X-ray source (1486.71 eV). Survey spectra (0-1100 eV) were taken at constant analyzer pass energy of 160 eV, and all high-resolution spectra for C_{1s} and O_{1s} were acquired with a pass energy of 20 eV, a step of 0.1 eV and a dwell time of 200 ms. The takeoff angles between the film surface and the photoelectron energy analyzer were of 90 degree. The typical operating pressure was around 5×10^{-10} Torr in the analysis chamber. The peaks were fit using the CasaXPS application software. The samples for XPS measurements were prepared from dropping 2 μL sample solution onto SPCE working electrode surface, drying in N_2 stream.

2.2. Preparation of graphene oxide

GO was prepared from graphite powder according to the modified Hummers method [35, 36]. Briefly, graphite powder (5 g) was oxidized by adding to a hot solution (80°C) of concentrated H_2SO_4 (30 mL) containing $K_2S_2O_8$ (10 g), and P_2O_5 (10 g). The resultant dark blue mixture was thermally isolated and slowly cooled to room temperature over a period of 6 h. The mixture was diluted to 300 mL and then filtrated with a 0.22 μm filter membrane (Generay Biotech Co., Ltd., Shanghai, China). The filtered product was dried overnight at 60°C. The pre-oxidized graphite powder (4 g) was added to 82 mL cold H_2SO_4 (0°C), and 12 g $KMnO_4$ was gradually added under stirring in ice-bath. The

resulted mixture was further stirred at 35ºC for 2 h and distilled water (200 mL) was added. The reaction was stopped with the addition of a mixture of 560 mL distilled water and 10 mL 30% H_2O_2. For purification, the mixture was washed with 1:10 HCl and then with water. The GO product was re-suspended in water to a brown dispersion, which was subjected to dialysis to remove residual metal ions and acids. The purified GO dispersion was sonicated for about 1.5 h to exfoliate GO, and un-exfoliated GO was removed by centrifugation (3000 rpm, 5 min). In order to obtain rGO, hydrazine hydrate was added to the GO dispersion and stirred at 80°C for about 1 h.

2.3. Preparation and modification of the electrode

The integrated three-electrode devices were mass manufactured by a screen-printing process using an AT-25P machine (ATMA CHAMP ENT. Corp.). The fabrication of SPCEs has been reported in our previous work [37]. On 0.5 mm thick glass fiber plate, as the substrate material, the circular working electrode (WE) (planar area: 3.1 mm^2, thickness: 15 μm) and the ring-shaped counter electrode were firstly fabricated from carbon ink and silver ink acting as conductive medium was printed as the second layer. The reference electrode was prepared with the silver-silver chloride ink. The insulating ink (Jelcon AC-3G, JUJO Chemical Co., Ltd., Japan) was used to provide the insulation layer which defines the thin-layer electrochemical micro-cell. The integrated three-electrode devices needed vacuum drying at 100ºC for 30 min after each step of the printing process. Finally, the integrated devices were vacuum dried at 140ºC for 90 min, then stored in vacuum container before use.

In order to modify the working electrode at the integrated SPCEs, the SPCEs was first washed with distilled water and dried by N_2 stream. Then the SPCEs was pre-anodized in a 0.1 M (pH = 7.4) PBS containing 0.1 M KCl by applying an anodic potential of +1.9 V (vs. Ag/AgCl) for 120 s [38]. The rGO/SPCEs (or GO/SPCEs) was prepared by coating 5 μL 0.3 mg/mL of the rGO (or GO) homogeneous suspension onto the SPCEs and then dried at room temperature overnight. All modified electrodes were cleaned by cyclic voltammetric technique between –0.5 and +0.5 V at a scan rate of 50 mV/s in PBS (pH 7.4) until a stable cyclic voltammetric response was obtained, and then rinsed with water and dried under a nitrogen stream.

3. RESULTS AND DISCUSSION

3.1. Characterization of GO (or rGO) modified SPCEs

Scanning Electron Microscope (SEM) could provide an image of the surface details, and produce the signals containing the information about the surface topography, composition and other properties. Fig. 1 presents the surface SEM images of bare SPCEs, rGO/SPCEs and GO/SPCEs. Some fractions on the SPCEs surface are exposed after the modification with rGO, which is due to the weak dispersion of rGO. However, GO could disperse very well in aqueous solution because of a large number of oxygen-containing groups on the surface, such as epoxy/ether group, the carbonyl carbon

and the carboxylate carbon. Thus, GO could be spread uniformly on the surface of SPCEs, which provides the large amount of edge plane sites for the electrocatalytic oxidation toward NADH.

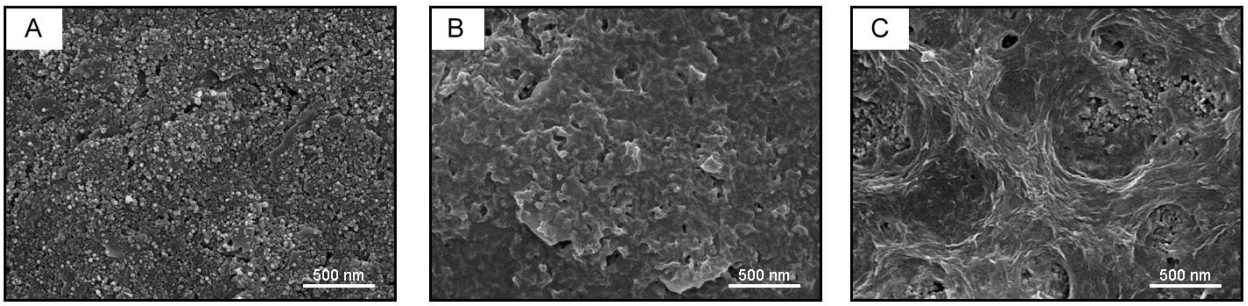

Figure 1. SEM images of SPCEs (A), GO/SPCEs (B) and rGO/SPCEs (C).

X-ray photoelectron spectroscopy (XPS) is a quantitative surface analysis technique that measures the elemental composition, empirical formula, chemical state and electronic state of the elements. The chemical composition of the bare SPCEs, GO/SPCEs and rGO/SPCEs were monitored by XPS. The high-resolution spectra for C_{1s} and O_{1s} are shown in Fig. 2A, B, C and E, F, D, respectively. The peak fitting of C_{1s} and O_{1s} spectra was applied the mixed Gaussian/Lorentzian function to fit peak shape after a Shirley background correction. The C_{1s} XPS spectra could be deconvoluted into five components corresponding to carbon atoms in different oxygen-containing functional groups[39]: (a) the non-oxygenated C at ~284.5 eV, (b) the carbon in C–O at ~285.5 eV, (c) the epoxy/ether group (C–O–C, ~286.5 eV), (d) the carbonyl carbon (C=O, ~288 eV), and (e) the carboxylate carbon (H–O–C=O, ~289 eV). The assignment of peak in O_{1s} spectra can further confirm the analysis information of C_{1s} components. The O_{1s} chemical shift at ~ 530.5 eV, ~532 eV and ~533.5 eV are assigned the contributions from C–O, C=O and H–O–C=O group, respectively. Table 1 shows the components of oxygen-containing functional groups on the surface of pre-anodized SPCEs, GO/SPCEs and rGO/SPCEs. A large number of oxygen-containing groups on the surface of the pre-anodized SPCEs and GO/SPCEs are observed (50.42 % and 52.23 % respectively), while it is greatly decreased to 36.02 % on the rGO/SPCEs surface. There is a significantly decreased component for the epoxy/ether groups (from 12.80 % to 11.12 %) and carbonyl groups (from 15.22 % to 3.59 %). All these results supported the hypothesis that epoxy/ether and hydroxyl/alkoxide groups are generated by the ring-opening reduction reaction of epoxides [40]. In addition, it could be further inferred that the edge plane sites contain a large number of oxygen-containing groups on the GO/SPCEs surface [41]. It has been reported that the oxidation of NADH is actually redox-mediated by such kind of oxygen-containing groups on the surface of some carbon materials, such as carbon nanotubes [42, 43], carbon nanofibers [44], and graphite [45]. The further CVs measurements were conducted to verify this conclusion as well.

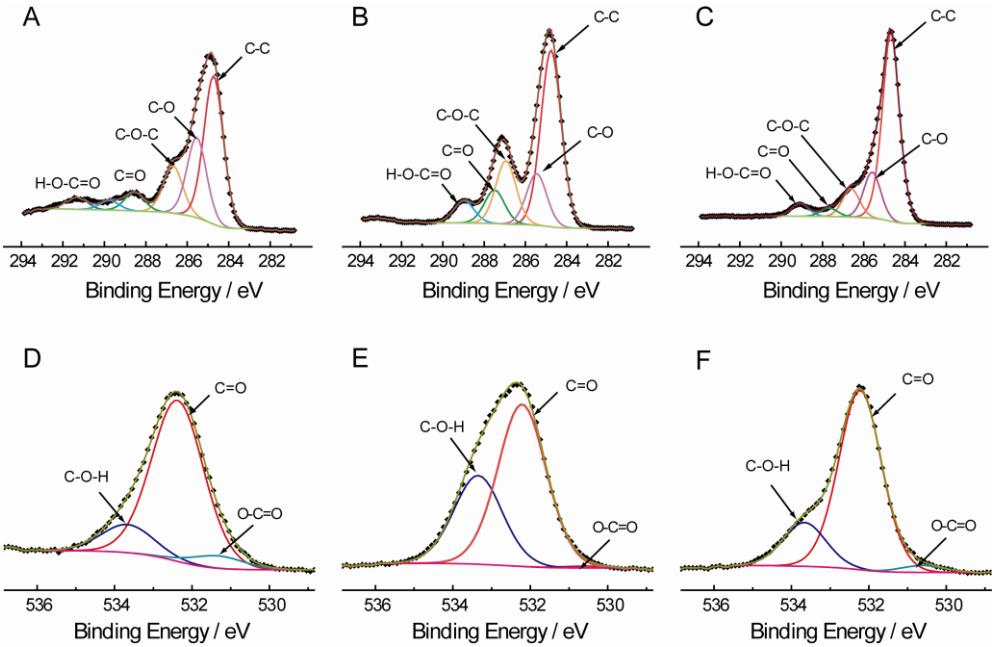

Figure 2. Deconvoluted the C_{1s} and O_{1s} XPS spectra of the pre-anodized SPCEs (A, D), GO/SPCEs (B, E) and rGO/SPCEs (C, F). Solid square symbol: experimental data; solid line: fitting curve.

Table 1. XPS spectra results for C_{1s} and O_{1s} in the samples of SPCE, GO/SPCEs and rGO/SPCEs.

		PRE-ANODIZED SPCES		GO/SPCES		RGO/SPCES	
	Group	Binding Energy (eV)	Area %	Binding Energy (eV)	Area %	Binding Energy (eV)	Area %
C_{1s}	C–C	284.7	46.56	284.7	47.77	284.6	63.98
	C–O	285.4	25.22	285.3	17.67	285.4	16.92
	C–O–C	286.6	14.92	286.7	12.80	286.4	11.12
	C=O	288.5	5.91	287.7	15.22	287.5	3.59
	H–O–C=O	289.6	3.02	288.9	6.54	289.0	4.40
O_{1s}	C–O	530.4	6.17	530.7	2.68	530.6	3.03
	C=O	532.3	79.87	532.2	42.97	532.2	77.93
	H–O–C=O	533.5	13.97	533.2	55.36	533.6	19.03

3.2. Electrocatalytic oxidation of NADH

The electrochemical performance of both GO/SPCEs and rGO/SPCEs towards the oxidation of NADH in PBS was investigated by cyclic voltammetry. As shown in Fig. 3, there is no electrocatalytic oxidation peak of NADH in the cyclic voltammograms (CVs) of bare SPCEs, GO/SPCEs and rGO/SPCEs in the absence of NADH in PBS. Interestingly, a couple of redox peaks in the CVs of

GO/SPCEs and rGO/SPCEs at a formal potential ($E_{1/2}$) of –0.07 V and –0.04 V were observed in background solution. These may be caused by the electrochemical redox of the oxygen-containing groups at the edge plane sites of GO and rGO, which could be supported by the components of C=O in the XPS C_{1s} spectrum (Table 1).

For the GO/SPCEs, as shown in Fig. 3B, a remarkable oxidation peak is observed starting around -0.1V with a peak at +0.41 V in the presence of 0.5 mM NADH in pH 7.4 PBS. The peak current of electrocatalytic oxidation of NADH at GO/SPCEs increases more significantly at +0.41V compared with SPCEs and rGO/SPCEs after the successive addition of NADH into the solution. However, the oxidation activity is observed at the SPCEs (Fig. 3A) and rGO/SPCEs (Fig. 3C) starting ca. 0.1 V and 0.05 V with peaks at +0.49 V and +0.51 V, respectively. Obviously, the oxidation peak potential at the GO/SPCEs is more negative than that at the bare SPCEs (Fig. 3A) and rGO/SPCEs (Fig. 3C), suggesting that the electron transfer kinetics for NADH oxidation on GO/SPCEs is essentially faster than the bare SPCEs and rGO/SPCEs. The effect of scan rates on electron transfer between NADH and the surface of electrode was evaluated (not shown). With an increasing scan rates, the anodic peak potential of NADH shifted to a more positive value, and the oxidation current were proportional to the square root of scan rates, indicating a diffusion-controlled behavior. From these demonstrations, we may conclude that the fast electron transfer kinetics for the NADH oxidation at the GO/SPCEs could be mainly associated with the presence of the oxygen-containing groups at this kind of carbon materials with edge plane sites.

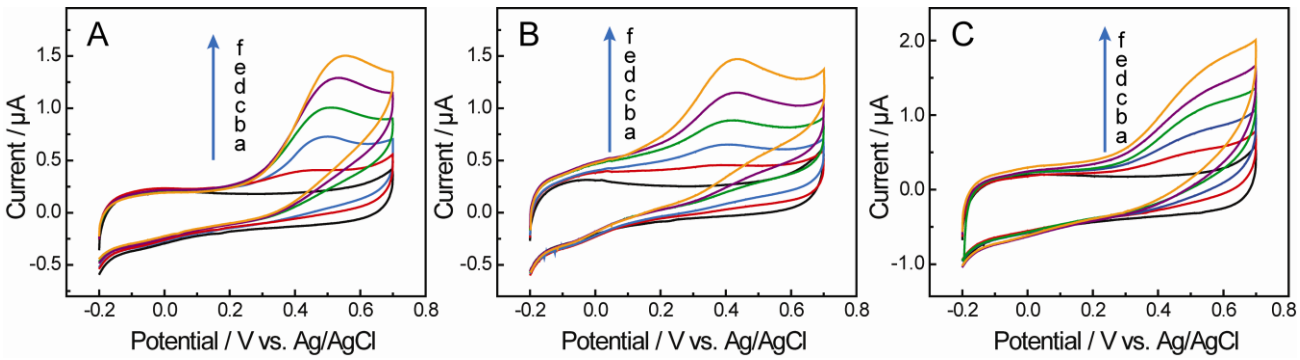

Figure 3. Cyclic voltammograms curves of SPCEs (A), GO/SPCEs (B) and rGO/SPCEs (C) in 0.1 M PBS containing various concentration of NADH, a), 0; b),0.1; c), 0.2; d), 0.3; e), 0.4; f), 0.5 mM, pH = 7.4, scan rates: 10 mV/s.

It is well known that ascorbic acid (AA) is an interference component during the electrochemical detection of NADH in biological samples. Furthermore, in order to eliminate the interference of ascorbic acid, electrodes can either be modified with anionic polymers or immobilize with ascorbate oxidase [46, 47]. However, modification with anionic polymers can also exclude NADH as it is negatively charged in neutral pH. The detection of NADH at the GO/SPCEs and rGO/SPCEs were examined in the presence of ascorbic acid in PBS. Fig. 4 shows the CV responses for equimolar concentration of ascorbic acid and NADH in pH 7.4 PBS. In the case of GO/SPCEs, there are two individual peaks at +0.13 and +0.41 V for ascorbic acid and NADH, respectively, with a peak

separation of over than 270 mV. In contrast, for the rGO/SPCEs, there are two small peaks at +0.22 V and +0.50 V respectively, which are not stable in the subsequent scan cycles. This suggests that the GO/SPCEs could be used to detect NADH and ascorbic acid simultaneously.

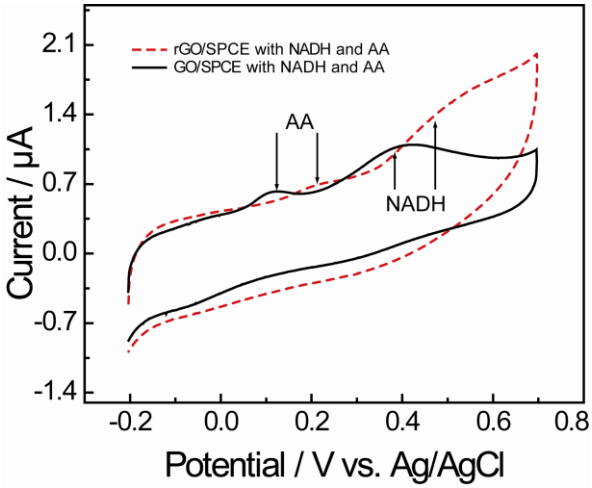

Figure 4. Cyclic voltammograms of the GO/SPCEs (solid line) and rGO/SPCEs (dot line) in 0.1 M PBS in the presence of 0.5 mM NADH and 0.5 mM AA. pH = 7.4, scan rate: 10 mV/s.

3.3. Amperometric detection of NADH

The electrochemical performance of GO/SPCEs towards the electrocatalytic oxidation of NADH in PBS (pH = 7.4) containing different concentration of NADH was investigated by the current–time response. As shown in Fig. 5A, a fast well-defined response was observed with the successive additions of NADH from 30 μM to 500 μM when the potential was applied at +0.40 V and the response current increased linearly with the additions of NADH. This experiment was repeated (Fig. 5A, insert) with trace additions over the linear range from 0.8 to 28.4 μM. The relationship (Fig. 5B) between the current and the concentration of NADH is following the linear equation: I/μA = 2.52*C*/mM + 0.31 (R^2 = 0.998), and a low limit of detection (LOD) of 0.10 μM was obtained (S/N = 3). In addition, it is worth to note that there is no significant electrode deactivation during continuous oxidation of NADH on the modified electrode, and the response time is less than one second, which is valuable in the development of NADH biosensor. The pre-anodized SPCEs was reported for the determination of NADH at the linear range of 10~500 μM with a LOD of 0.15 μM [26]. The carbon nanofibers (linear range: 0.2~686 μM / LOD: 0.11 μM), the carbon nanotubes (linear range: 20~5000 μM / LOD: 0.5 μM) and the highly oriented pyrolytic graphite (LOD, 0.3 μM) could also reach low detect limit respectively [33, 48, 49]. By contrast, the GO/SPCEs could present the excellent analytical performance in the determination of NADH. The *in-situ* UV-Vis spectroelectrochemical measurement was performed to further confirm the electrocatalysis oxidation of NADH at GO/SPCE in PBS. As shown in Fig. 5C, with applying the constant potential at 0.4 V, the UV-Vis spectra of NADH were recorded simultaneously. The absorbance peak, which is the characteristic band of NADH located at 340 nm, was gradually decreasing and with the time and disappeared after 90s. At the same time,

absorbance peak at 259 nm was increased slightly, which is present of the formation of NAD^+. The results provided the evidence of the oxidation process of NADH to NAD^+.

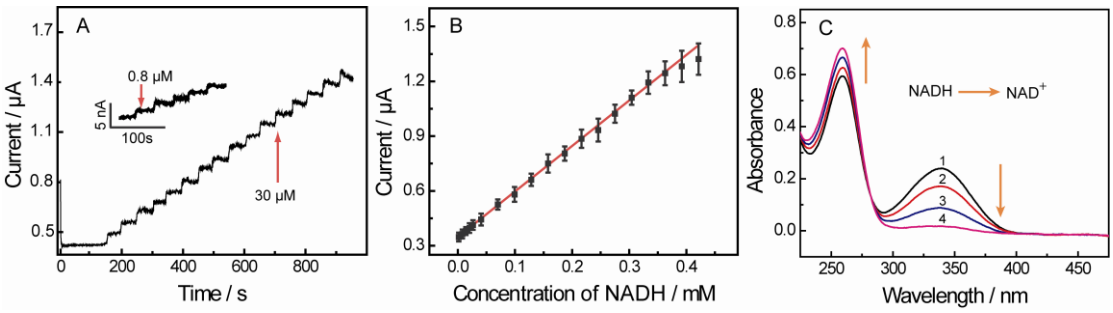

Figure 5. (A) Current–time curves of GO/SPCEs in PBS with various concentration of NADH, (B) The liner relationship of electrocatalytic oxidation current and concentration. (C) Real-time UV-vis spectrum of 0.2 mM NADH at different time, curve 1: 0s; curve 2: 10s; curve 3: 30s; curve 4: 90s. PBS: pH 7.4, applied potential: 0.4 V.

3.4 Stability of the biosensor

Long-term stability is one of the most important properties for biosensor application. The stability of GO/SPCEs was investigated by cyclic voltammetry. The response currents can retain almost constant upon continuous 20 cyclic sweeps over the applied potential ranging from −0.2 to +0.7 V with the scan rate of 10 mV/s. After stored in refrigerator at 4 °C for 90 days, the potentials of oxidation peak in CVs remained at the same positions and the peak currents decreased by only about 3.3% of its initial current response.

4. CONCLUSIONS

The present investigation reveals that the GO/SPCEs shows excellent electrocatalytic oxidation activity towards NADH with a remarkable decrease in overpotential and enhanced stability compared to the performance observed at a bare SPCEs and rGO/SPCEs. This could be attributed to the oxygen-containing functional groups on the surface of SPCEs, rGO/SPCEs and GO/SPCEs. The results of XPS provide a solid support to the oxygen-containing groups of edge plane sites on the surface of SPCEs, rGO/SPCEs and GO/SPCEs. The disposable SPCEs could act as the edge plane graphite electrode in the electrocatalytic oxidation of NADH. The detection range of GO/SPCEs is 0.8 to 500 μM with a lower detection limit of 0.10 μM. These facts offer a boarder application in the disposable amperometric NADH biosensors with immobilizing GO on the SPCEs surface.

ACKNOWLEDGEMENTS
The authors greatly appreciate the funding support from the Ministry of Health of China (No. 2009ZX10004-301), the National Natural Science Foundation of China (21001004). YTL thanks the

Program for Professor of Special Appointment (Eastern Scholar) at Shanghai Institutions of Higher Learning.

References

1. A.L. Lehninger, D. L. Nelson, M. M. Cox, Lehninger principles of biochemistry 5th edn: W.H. Freeman; (2008)
2. A.Radoi, D. Compagnone, *Bioelectrochem.* 76 (2009) 126.
3. H. Jaegfeldt, *J. Electroanal. Chem*. 110 (1980) 295
4. J. Moiroux, P. J. Elving, *Anal. Chem*. 50 (1978) 1056.
5. M. A. Hayes, W. G. Kuhr, *Anal. Chem.* 71 (1999) 1720.
6. F. Pariente, F. Tobalina, M. Darder, E. Lorenzo, H. D. Abruña, *Anal. Chem*. 68 (1996) 3135.
7. D. C. -S Tse, T. Kuwana, *Anal. Chem*. 50 (1978) 1315.
8. K. Hajizadeh, H. T. Tang, H. B. Halsall, W. R. Heineman, *Anal. Lett*. 24 (1991) 1453.
9. A.Kitani, Y. H. So, L. L. Miller, *J. Am. Chem. Soc*. 103 (1981) 7636.
10. T. Matsue, M. Suda, I. Uchida, T. Kato, U. Akiba, T. Osa, *J. Electroanal. Chem*. 234 (1987) 163.
11. M. Somasundrum, J. Hall, J. V. Bannister, *Anal. Chim. Acta* 295 (1994) 47.
12. C. Ueda, D. C.-S Tse, T. Kuwana, *Anal. Chem.* 54 (1982) 850.
13. A.Torstensson, L. Gorton, *J. Electroanal. Chem*. 130 (1981) 199.
14. P. Norouzi, F. Faridbod, H. Rashedi, M. R. Ganjali, *Int. J. Electrochem. Sci.* 5 (2010) 1713.
15. R. R. Moore, C. E. Banks, R. G. Compton, *Anal. Chem*. 76 (2004) 2677.
16. L. N. Wu, X. J. Zhang, H. X. Ju, *Anal. Chem*. 79 (2007) 453.
17. A. Arvinte, F. Valentini, A. Radoi, F. Arduini, E. Tamburri, L. Rotariu, G. Palleschi, C. Bala, *Electroanalysis* 19 (2007) 1455.
18. B. Pérez, M. del Valle, S. Alegret, A. Merkoçi, *Talanta* 74 (2007) 398.
19. J. Wang, M. Musameh, *Anal. Chem*. 75 (2003) 2075.
20. Z. Liu, A. Fan, S. Sherlock, A. Goodwin, X. Chen, Q. Yang, D. Felsher, H. Dai, *Angew. Chem. Int. Engl*. 48 (2009) 7668.
21. M. Musameh, J. Wang, A. Merkoci, Y. H. Lin, *Electrochem. Commun*. 4 (2002) 743.
22. O. D. Renedo, M. A. Alonso-Lomillo, M. J. A. Martinez, *Talanta* 73 (2007) 202.
23. P. Norouzi, F. Faridbod, B. Larijani, M. R. Ganjali, *Int. J. Electrochem. Sci.* 5 (2010) 1213.
24. Q. Gao, X. Q. Cui, F. Yang, Y. Ma, X. R. Yang, *Biosens. Bioelectron*. 19 (2003) 277.
25. H. R. Zarea, N. Nasirizadeh, *Int. J. Electrochem. Sci.,* 4 (2009) 1691.
26. A. S. Adekunle1, K. I. Ozoemena, *Int. J. Electrochem. Sci.*, 5 (2010) 1726.
27. K. S. Prasad, J. C. Chen, C. Ay, J. M. Zen, *Sensors and Actuators B: Chem*. 123 (2007) 715.
28. C. Liu, S. Alwarappan, Z. Chen, X. Kong, C. Z. Li, *Biosens. Bioelectron*. 25 (2010) 1829.
29. S. He, B. Song, D. Li, C. Zhu, W. Qi, Y. Wen, L. Wang, S. Song, H. Fang, C. Fan, *Adv. Funct. Mater.* 20 (2010) 453.
30. S. Alwarappan, C. Liu, A. Kumar, C. Z. Li, *J. Phys. Chem.* C, 114 (2010) 12920.
31. K. E. Toghill, R. G. Compton, *Int. J. Electrochem. Sci.* 5 (2010) 1246.
32. X. Zuo, S. He, D. Li, C. Peng, Q. Huang, S. Song, C. Fan, *Langmuir*, 26 (2010) 1936.
33. C. E. Banks, R. G. Compton, *Analyst* 130 (2005) 1232.
34. P. N. Bartlett, E. N. K. Wallace, *J. Electroanal. Chem*. 486 (2000) 23.
35. W. S. Hummers, R. E. Offeman, *J. Am. Chem. Soc*. 80 (1958) 1339.
36. N. I. Kovtyukhova, P. J. Ollivier, B. R. Martin, T. E. Mallouk, S. A. Chizhik, E. V. Buzaneva, A. D. Gorchinskiy, *Chem. Mater*. 11 (1999) 771.
37. L. Zhang, D. W. Li, W. Song, L. Shi, Y. Li, Y. T. Long, *Sensors Journal*, IEEE **10** (2010) 1583.
38. J. Wang, M. Pedrero, H. Sakslund, O. Hammerich, J. Pingarron, *Analyst* 121 (1996) 345.
39. S. Park, K. S. Lee, G. Bozoklu, W. Cai, S. T. Nguyen, R. S. Ruoff', *Acs. Nano* 2 (2008) 572.

40. O. C Compton, S. T. Nguyen, *Small* 6 (2010) 711.
41. J. F. Wang, S. L. Yang, D. Y. Guo, P. Yu, D. Li, J. S. Ye, L. Q. Mao, *Electrochem. Commun*. 11 (2009) 1892.
42. L. D. Zhu, J. G. Zhai, R. L. Yang, C. Y. Tian, L. P. Guo, *Biosens. Bioelectron*. 22 (2007) 2768.
43. D. W. Yang, H. H. Liu, *Biosens. Bioelectron*. 25 (2009) 733.
44. F. Pariente, E. Lorenzo, F. Tobalina, H. D. Abruna, *Anal. Chem*. 67 (1995) 3936.
45. F. Pariente, F. Tobalina, G. Moreno, L. Hernández, E. Lorenzo, H. D. Abruña, *Anal. Chem*. 69 (1997) 4065.
46. J. Chen, J. C. Bao, C. X. Cai, T. H. Lu, *Anal. Chim. Acta* 516 (2004) 29.